Am J Transl Res 2021;13(12):13406-13422
www.ajtr.org /ISSN:1943-8141/AJTR0138204

*Original Article*

# CDKN2B-AS1 promotes the proliferation, clone formation, and invasion of nasopharyngeal carcinoma cells by regulating miR-98-5p/E2F2 axis

Zhengwen Li, Xiaojing Cai, Wentao Zou, Jiaxiong Zhang

*Department of Otorhinolaryngology, Shanghai Tenth Peoples' Hospital, Tongji University, Shanghai 200072, China*

Received August 11, 2021; Accepted October 19, 2021; Epub December 15, 2021; Published December 30, 2021

**Abstract:** Objective: To explore the effect of CDKN2B antisense RNA 1 (CDKN2B-AS1) on the proliferation, clone formation, and invasion of nasopharyngeal carcinoma (NPC) cells by regulating miR-98-5p/E2F transcription factor 2 (E2F2) axis. Methods: The expressions of CDKN2B-AS1, miR-98-5p, and E2F2 in NPC tissues and cell lines (SUNE-1, 5-8F, 6-10B, and HK-1) as well as in peritumoral normal tissues and cell line NP69 were determined by qRT-PCR. Subcellular localization of CDKN2B-AS1 was detected using the fluorescence *in situ* hybridization assay. The targeting relationships between CDKN2B-AS1 and miR-98-5p as well as between miR-98-5p and E2F2 were analyzed by the dual-luciferase reporter assay and RNA binding protein immunoprecipitation assay. The proliferation, clone formation and invasion of 5-8F cells were measured using the CCK-8 assay, Clone formation assay, and transwell assay, respectively. Results: CDKN2B-AS1 was highly expressed in NPC tissues and cells, whereas the expression of miR-98-5p decreased in the NPC tissues and cells. Silencing of CDKN2B-AS1 inhibited the proliferation, clone formation, and invasion of NPC cells (all $P<0.05$). CDKN2B-AS1 acted asceRNA of miR-98-5p, and miR-98-5p inhibitor could partially reverse the inhibitory effect of silencing CDKN2B-AS1 on NPC cells (all $P<0.05$). CDKN2B-AS1 upregulated E2F2 by inhibiting miR-98-5p, and the upregulation of E2F2 partially reversed the inhibitory effect of miR-98-5p overexpression on the NPC cells (all $P<0.05$). Conclusion: CDKN2B-AS1, as a lncRNA, can regulate E2F2 by sponging miR-98-5p to promote the proliferation, clone formation, and invasion of NPC cells.

**Keywords:** CDKN2B-AS1, miR-98-5p, E2F2, nasopharyngeal carcinoma

## Introduction

Nasopharyngeal carcinoma (NPC) is a highly prevalent head and neck cancer. The tumor is mainly located on the lateral wall and the top of the nasopharyngeal cavity [1, 2]. The incidence of NPC in Southeast Asia is high, and that region accounts for 40% of the new cases worldwide every year. Although the combination of magnetic resonance imaging, intensity-modulated radiotherapy, and concurrent chemotherapy can significantly improve the prognosis of NPC, about 30% of NPC patients can still experience recurrence or tumor metastasis [3-5]. Hence, it is of great significance to identify the predictive biomarkers and elucidate the mechanism of the disease for developing individualized therapy for NPC.

NPC treatment depends on accurate prognosis, and the tumor metastasis (TNM) staging system has been implemented currently as guidance for treatment [6]. According to TNM staging, patients with NPC can be classified into four stages to receive stratified treatment. However, studies have reported that even though patients with NPC at the same stage receive similar treatment, the clinical outcome can vary among them. This finding indicates that TNM staging cannot fully reveal the biologic heterogeneity of tumors and cannot accurately predict the risks for treatment failure in patients with NPC. Therefore, in order to solve the limitation of TNM staging, various biomarkers, including EBV-DNA, miRNA, and gene profiling, have been suggested to predict prognosis of NPC. However, more studies need to be conducted to verify biomarkers and treatment targets.

Long non-coding RNA (lncRNA), which is over 200 nucleotides in length, is a subclass of non-

**Table 1.** Primer sequences

| Gene | Primer | Sequence (5'-3') |
|---|---|---|
| CDKN2B-AS1 | Forward | CAACCTTGAACTCCCAGGCTC |
| | Reverse | TGGCCAATCTGCAGTTTGTCT |
| miR-98-5p | Forward | TGAGGTAGTAGTTTGTGCTGTT |
| | Reverse | GCGAGCACAGAATTAATACGAC |
| E2F2 | Forward | CCGACTTCCACAGAGTGCTTCA |
| | Reverse | GCTCGTGCCTGTCATCTCAACA |
| GAPDH | Forward | ACCACAGTCCATGCCATCAC |
| | Reverse | TCCACCACCCTGTTGCTGTA |
| U6 | Forward | GCUUCGGCAGCACAUAUACUAAAAU |
| | Reverse | CGCUUCACGAAUUUGCGUGUCAU |

Note: CDKN2B-AS1: CDKN2B antisense RNA 1; E2F2: E2F transcription factor 2.

coding RNA [7, 8]. In recent years, it has been found that the aberrant regulation of lncRNA serves an essential role in the pathogenesis of NPC. For instance, lncRNA HOXA-AS2 can promote NPC progression by sponging miR-519 [9]. CCHE1 can enhance the proliferation, migration, and invasion of NPC cells by inhibiting the MEK/ERK/c-Myc pathway [10]. However, research on the role of lncRNAs in tumorigenesis, especially on progression of NPC, is still in the early stages. Therefore, elucidating the mechanism of lncRNA-mediated gene regulation is essential to identify prognostic markers for NPC and guide individualized treatment.

According to the lncRNA disease database, it has been reported that the single nucleotide polymorphism (rs3217992, A>G; rs1063192, C>T) on CDKN2B antisense RNA 1 (CDKN2B-AS1) can increase the susceptibility to NPC [11, 12]. Thus, we speculated that inhibiting CDKN2B-AS1 expression may affect the progression of NPC. In addition, it has been revealed that CDKN2B-AS1 is highly expressed in advanced NPC and the knockdown of CDKN2B-AS1 can significantly suppress the proliferation and transformation of NPC cells. CDKN2B-AS1 can promote the malignant progression of NPC by inducing the proliferation of the cancer cells and reprogramming glucose metabolism in cells [13]. In this study, we speculated that CDKN2B-AS1 may be a treatment target for NPC, and the mechanism of CDKN2B-AS1 in NPC needs to be further investigated.

lncRNA can indirectly regulate gene coding by sponging miRNA, thus affecting the downstream gene expression. We first used the bioinformatics tool to identify the miRNAs to which CDKN2B-AS1 binds. Based on relevant literature, we then chose miR-98-5p for this study. miR-98-5p has been widely studied in different cancers including lung cancer, liver cancer, and prostate cancer and has been demonstrated to exert an anti-cancer effect [14-16]. However, there have been no reports on the anti-cancer effect of miR-98-5p in NPC. We speculated that miR-98-5p and CDKN2B-AS1 may participate in NPC progression at the same time.

Subsequently, we searched the bioinformatics database to find the possible downstream targets of miR-98-5p. After conducting Gene Ontology (GO) and pathway analysis, E2F transcription factor 2 (E2F2) was identified. E2F2, as an E2F family member, can regulate cell proliferation and division and is closely correlated with the cancer cell activity of various tumors and cancer progression [17]. Therefore, we speculated that miR-98-5p may regulate tumor growth by suppressing E2F2.

We aimed to investigate the effect of the CDKN2B-AS1/miR-98-5p/E2F2 axis on cell proliferation, clone formation, and invasion of NPC cells, to find treatment targets and prognostic markers for NPC patients.

## Materials and methods

### *Bioinformatic tools*

The following tools were used in this study: (1) starBase (http://starbase.sysu.edu.cn/starbase2/) and lncRBase (http://carolina.imis.athena-innovation.gr/diana_tools/web/index.php?r=lncbasev2/index) for predicting the miRNA-lncRNA interactions; (2) RNA22 (http://cm.jefferson.edu/rna22/) and miRWalk (http://mirwalk.umm.uni-heidelberg.de/) for predicting miRNA target genes; (3) Venny (https://bioinfogp.cnb.csic.es/tools/venny/index.html) for plotting Venn diagram; (4) DAVID (https://david.ncifcrf.gov/) for GO enrichment and pathway enrichment analysis; (5) ggplot2 for creating bubble chart for GO enrichment and pathway enrichment analysis; (6) DisGeNET database (https://www.disgenet.org/) for finding published disease genes; (7) string database

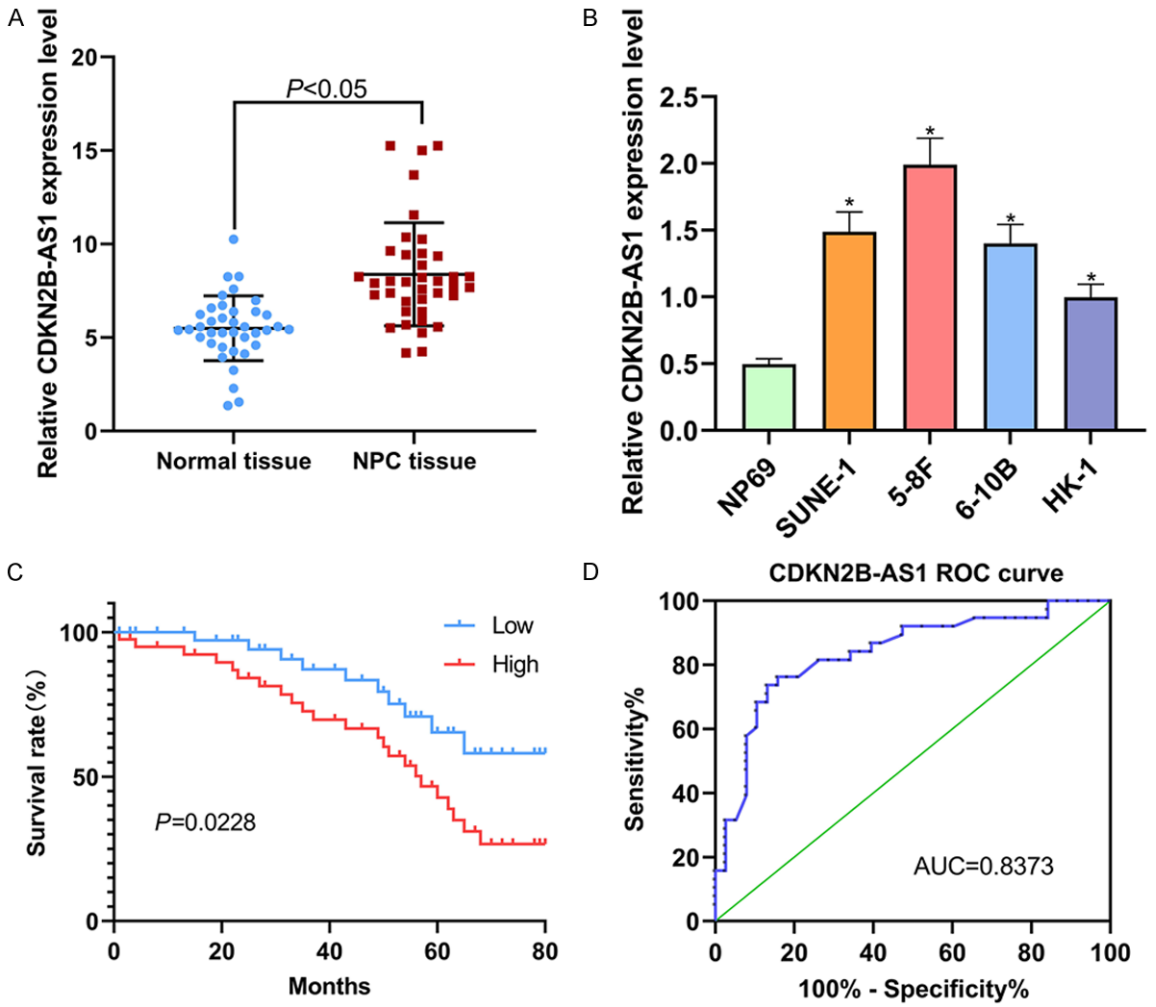


**Figure 1.** Expression level of CDKN2B-AS1. A: Relative expression levels of CDKN2B-AS1 in NPC tissues (n=38); B: Relative expression levels of CDKN2B-AS1 in normal cells and NPC cells; C: Kaplan-Meier overall survival curve in association with the CDKN2B-AS1 expression levels; D: ROC curve of CDKN2B-AS1 in the diagnosis of NPC. Compared to the cell line NP69, *P<0.05. CDKN2B-AS1: CDKN2B antisense RNA 1; NPC: nasopharyngeal carcinoma; ROC: receiver operating characteristic.

(https://string-db.org/) for finding the interactions between the candidate genes and disease risk genes on the protein level.

*Tissue collection*

Thirty-eight fresh frozen NPC tissues and normal peritumoral nasopharynx tissues (2-5 cm away from the tumor edge) were collected from the patients admitted in our hospital between June 2018 and February 2020. Their tissue samples were kept at -80°C.

*Inclusion criteria:* (1) Patients pathologically diagnosed with NPC; (2) Patients who did not receive any anti-tumor treatment before the surgery; (3) Patients diagnosed with NPC for the first time.

*Exclusion criteria:* Patients with other types of tumors, immune system diseases, or heart, liver, or kidney dysfunction.

The study was approved by the Ethics Committee of our hospital (approval number 2021KN176), and all participants signed a written informed consent.

*Cell culture*

Human immortalized nasopharyngeal epithelial cell line (NP69, ATCC, USA) and NPC cell

**Table 2.** Effect of expression levels of CDKN2B-AS1 on the clinical characteristics of patients with NPC (n=38)

| Characteristic | Case (n=38) | CDKN2B-AS1 low expression (n=7) | CDKN2B-AS1 high expression (n=31) | P |
|---|---|---|---|---|
| Gender | | | | |
| Male | 21 | 5 | 16 | 0.4267 |
| Female | 17 | 2 | 15 | |
| Age (years old) | | | | |
| <55 | 25 | 8 | 17 | 0.2955 |
| ≥55 | 13 | 3 | 10 | |
| TNM stage | | | | |
| I-II | 18 | 6 | 12 | 0.0381 |
| III-IV | 20 | 1 | 19 | |
| EA-IgA positive | | | | |
| <1:10 | 15 | 2 | 13 | 0.6807 |
| ≥1:10 | 23 | 5 | 18 | |
| VCA-IgA positive | | | | |
| <1:80 | 7 | 45 | 2 | 0.0008 |
| ≥1:80 | 31 | 2 | 29 | |
| Pathological type | | | | |
| Non-keratinizing | 33 | 5 | 28 | 0.2227 |
| Keratinizing | 5 | 2 | 3 | |
| Lymphatic metastasis | | | | |
| No | 12 | 6 | 6 | 0.0020 |
| Yes | 26 | 1 | 25 | |

Note: CDKN2B-AS1: CDKN2B antisense RNA 1; NPC: nasopharyngeal carcinoma; TNM: tumor metastasis.

lines (SUNE-1, 5-8F, 6-10B, and HK-1, ATCC, USA) were cultured in RPMI1640 medium (Solarbio Science & Technology, Beijing, China) containing 10% fetal bovine serum and placed in a humidified incubator at 37°C in 5% $CO_2$.

*Grouping and transfection*

According to the manufacturer's instructions, vectors and control vectors were constructed after regulating the levels of CDKN2B-AS1, miR-98-5p, and E2F2 in the NPC cells. The cells were divided into the following groups: blank group (blank control), si-NC group (5-8F cells transfected with a negative control sequence of si-CDKN2B-AS1), miR-NC group (5-8F cells transfected with a negative control sequence of miR-98-5p), si-CDKN2B-AS1 group (5-8F cells transfected with si-CDKN2B-AS1), miR-98-5p mimic group (5-8F cells transfected with miR-98-5p mimic), si-CDKN2B-AS1 + miR-NC group (5-8f cells transfected with si-CDKN2B-AS1 and miR-NC), si-CDKN2B-AS1 + miR-inhibitor group (5-8f cells transfected with si-CDKN2B-AS1 and miR-98-5p inhibitor), miR-98-5p mimic + E2F2 group (5-8F cells transfected with miR-98-5p mimic and pcDNA3.1-E2F2), and miR-98-5p mimic + vector group (5-8F cells transfected with miR-98-5p mimic and blank vector).

The sequences and transfection vectors were from GenePharma, Shanghai, China. The cells in each group were transfected using Lipofectamine™ 3000 (Thermo Fisher Scientific, USA) in accordance with the manufacturer's protocol. To construct the E2F2 overexpression vector, the cDNA was amplified and cloned into the pcDNA3.1 vector, and the empty vector was the negative control. Other transfection sequences used in the experiment were: si-CDKN2B-AS1 (5'-GUGCGUACAGUGCUGUACAGCAU-3'), si-NC (5'-UACGCUCAGCAUGUGUCACUC-3'), miR-98-5p mimic (5'-UCGUUCGUGAGCACUUGCGACG-3'), miR-inhibitor (5'-AGCCUUGCUGCAGGUGCGCAU-3'), and miR-NC (5'-UGCCUUACUGACGGUCGGAGA-3').

*qRT-PCR*

The total RNA was isolated from the tissue samples and the cells using the Trizol reagent (Beyotime Biotechnology, Shanghai, China). The purity and concentration of the RNAs were determined with the UV spectrophotometer (Lab-Spectrum Instruments, Shanghai, China). The RNAs were reverse transcribed into cDNAs following the manufacturer's protocol of the one-step reverse transcription kit (Solarbio Science & Technology, Beijing, China). The reaction system and conditions of PCR were set up according to the manufacturer's instructions of real-time quantitative PCR kit (Takara, Japan). The relative expression level of the genes was calculated using the $2^{-\Delta\Delta Ct}$ method

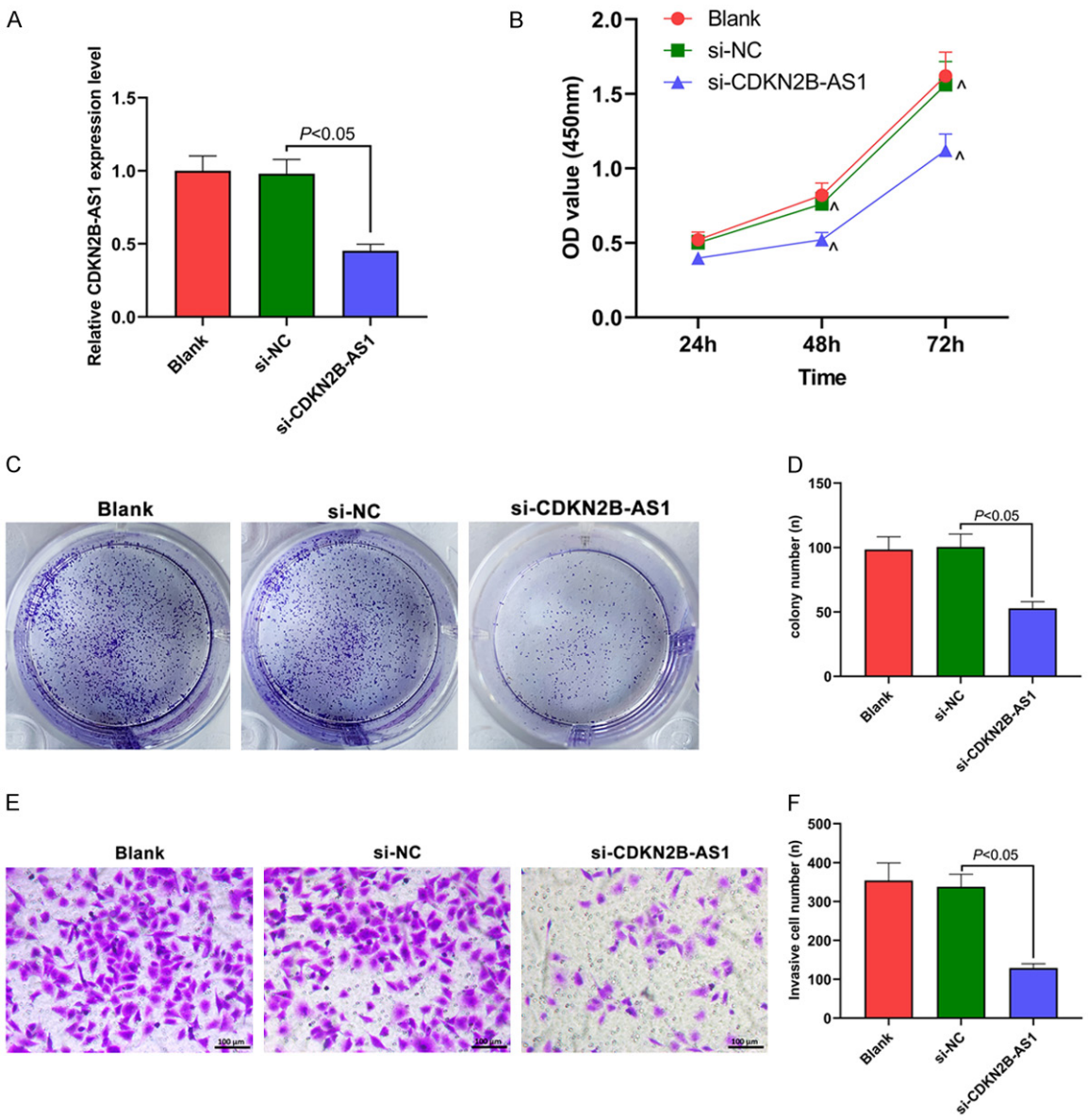


**Figure 2.** Effect of CDKN2B-AS1 knockdown on NPC cells. A: Knockdown efficiency of CDKN2B-AS1; B: Cell proliferation measured by CCK-8 assay; C, D: Results of clone formation; E, F: Cell invasion measured by Transwell assay (100×). Compared to the si-NC group, ^P<0.05. CDKN2B-AS1: CDKN2B antisense RNA 1; NPC: nasopharyngeal carcinoma; CCK-8: cell counting kit-8; OD: optical density.

with U6 as the internal reference for miRNA and GAPDH as the internal reference for lncRNA and mRNA. The primers are displayed in **Table 1**.

*Cell counting kit-8 (CCK-8) assay*

The cells were seeded into a 96-well plate (1*$10^3$ per well), and 10 μL of CCK-8 solution (Beyotime Biotechnology, Shanghai, China) was added into each well at 24 h, 48 h, and 72 h. The cells were then incubated at 37°C for 2 h. The optical density was measured at 450 nm.

*Clone formation assay*

The NPC cells were inoculated into a 6-well plate (1*$10^3$ per well) and incubated at 37°C for 15 days. Afterward, the cells were washed in PBS (Beyotime Biotechnology, Shanghai, China) and fixed with 4% paraformaldehyde (Beyotime Biotechnology, Shanghai, China) followed by

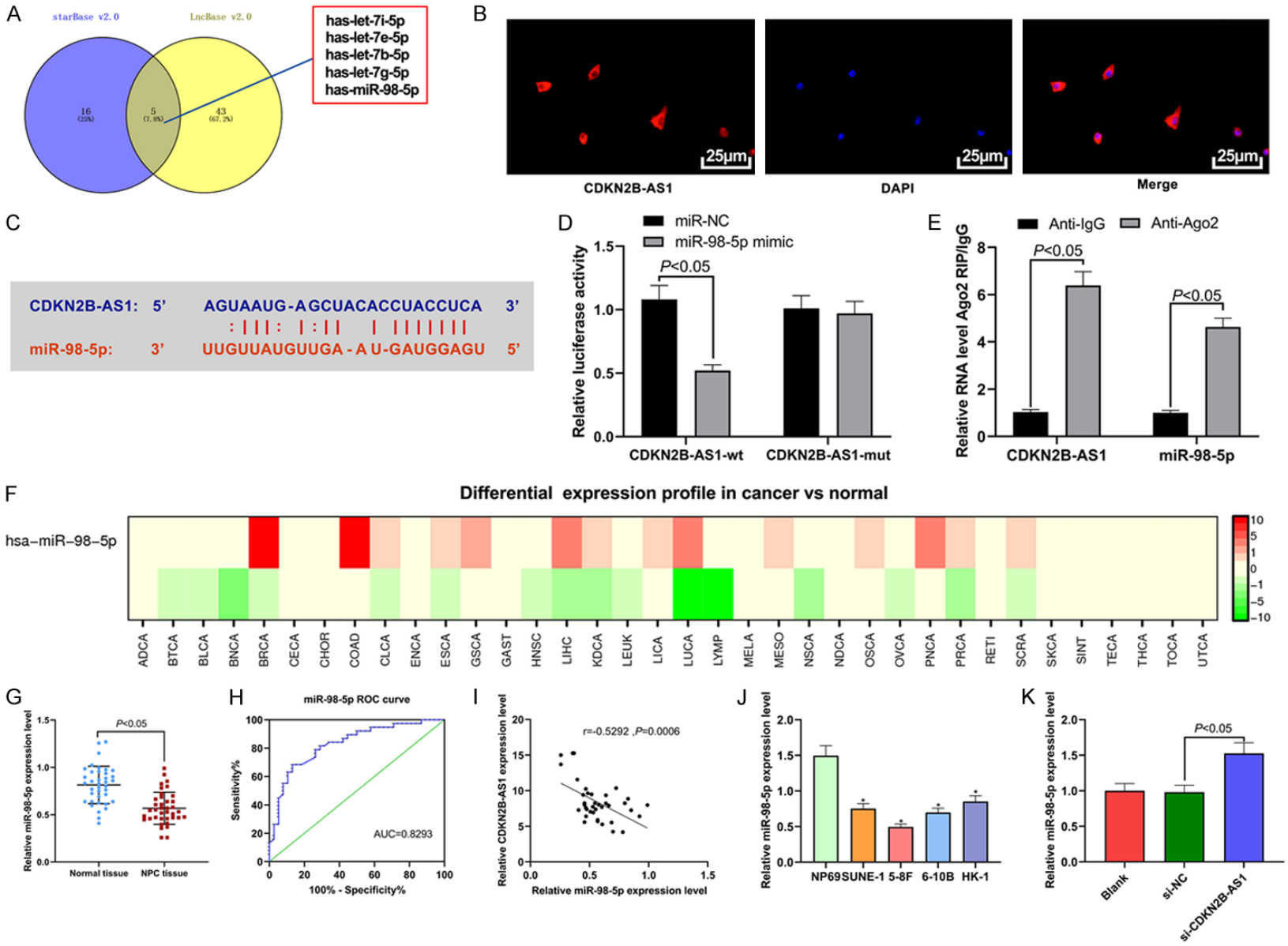
A
starBase v2.0
LncBase v2.0
16
(25%)
5
(7.8%)
43
(67.2%)
has-let-7i-5p
has-let-7e-5p
has-let-7b-5p
has-let-7g-5p
has-miR-98-5p
B
25μm
CDKN2B-AS1
DAPI
Merge
C
CDKN2B-AS1: 5' AGUAAUG-AGCUACACCUACCUCA 3'
miR-98-5p: 3' UUGUUAUGUUGA-AU-GAUGGAGU 5'
D
miR-NC
miR-98-5p mimic
Relative luciferase activity
P<0.05
CDKN2B-AS1-wt
CDKN2B-AS1-mut
E
Anti-IgG
Anti-Ago2
Relative RNA level Ago2 RIP/IgG
P<0.05
P<0.05
CDKN2B-AS1
miR-98-5p
F
Differential expression profile in cancer vs normal
hsa-miR-98-5p
ADCA BTCA BLCA BNCA BRCA CECA CHOR COAD CLCA ENCA ESCA GSCA GAST HNSC LIHC KDCA LEUK LICA LUCA LYMP MELA MESO NSCA NDCA OSCA OVCA PNCA PRCA RETI SCRA SKCA SINT TECA THCA TOCA UTCA
G
Relative miR-98-5p expression level
P<0.05
Normal tissue
NPC tissue
H
miR-98-5p ROC curve
Sensitivity%
AUC=0.8293
100% - Specificity%
I
Relative CDKN2B-AS1 expression level
r=-0.5292 ,P=0.0006
Relative miR-98-5p expression level
J
Relative miR-98-5p expression level
NP69 SUNE-1 5-8F 6-10B HK-1
K
Relative miR-98-5p expression level
P<0.05
Blank
si-NC
si-CDKN2B-AS1

**Figure 3.** miR-98-5p is a target of CDKN2B-AS1. A: The common miRNA binding sites on CDKN2B-AS1 predicted by starBase and lncRBase; B: Subcellular localization of CDKN2B-AS1 detected by FISH assay (400×); C: miR-98-5p binding sites on CDKN2B-AS1; D: DLR assay results; E: RIP assay results; F: Expression levels of miR-98-5p in various tumors; G: Expression levels of miR-98-tp in the NPC tissues (n=38); H: ROC curve of miR-98-5p in the diagnosis of NPC; I: Correlation between the expression level of CDKN2B-AS1 and the expression level of miR-98-5p; J: Expression of miR-98-5p in the NPC cell line; K: Expression level of miR-980tp in NPC. Compared with the NP69 cell line, *P<0.05. CDKN2B-AS1: CDKN2B antisense RNA 1; NPC: nasopharyngeal carcinoma; OD: optical density; FISH: fluorescence in situ hybridization; DLR: dual-luciferase reporter; RIP: RNA immunoprecipitation.

hematoxylin staining. The cell colonies were observed and photographed under a microscope (Olympus, Japan).

*Transwell assay*

The upper side of the Transwell insert was precoated with Matrigel (Solarbio Science & Technology, Beijing, China) and 200 of μL serum-free medium (N6010, Solarbio Science & Technology, Beijing, China) containing $1*10^5$ cells was added to the insert. Meanwhile, 600 μL of RPMI1640 medium (Solarbio Science & Technology, Beijing, China) containing 10% fetal bovine serum was placed in the lower chamber. The cells were incubated at 37°C in 5% $CO_2$ for 24 hours. The non-invasive cells were removed from the Transwell upper chamber. After being fixed with 4% paraformaldehyde (Beyotime Biotechnology, Shanghai, China) and stained with hematoxylin, the invading cells were observed and counted under an optical microscope (Olympus, Japan).

*Fluorescence in situ hybridization (FISH)*

The subcellular localization of CDKN2B-AS1 was detected using the FISH kit (BersinBio, Guangzhou, China). According to the manufacturer's protocol, the cells were first incubated in a 24-well plate covered by a glass cover slide for 24 hours. After immobilization and infiltration, the cells were hybridized with CDKN2B-AS1 or U6-FISH probe mix (ribbio) labeled with 20 μm of Cy3. Next, the cells were stained with DAPI and observed under a confocal laser scanning microscope.

*RNA immunoprecipitation (RIP)*

The EZ-Magna RIP kit (Haoran Biotechnology, Shanghai, China) was used for RNA detection. According to the manufacturer's instructions, the cells at 24 h of transfection were collected with Ago2 antibody for RIP assay. IgG was used as the negative control, and the coprecipitated RNA was determined by qRT-PCR.

*Dual-luciferase reporter (DLR) assay*

The full-length sequences of CDKN2B-AS1 and E2F2 3'-UTR with or without mutant mir-98-5p binding site were cloned into pmiR-reporter plasmids. Afterward, the wild type and mutant reporter plasmids along with miR-98-5p mimic or control vectors were co-transfected into the NPC cells. At 48 h of transfection, the luciferase activity of the NPC cells was detected using the DLR assay kit (Solarbio Science & Technology, Beijing, China).

*Statistical analysis*

SPSS (18.0) was used for statistical analysis. Measured data are expressed as mean ± standard deviation. Independent samples t-test was performed for comparison between two groups; one-way analysis of variance was performed for comparison among multiple groups; LSD test was performed for pairwise comparison among multiple groups. Counted data were analyzed by Fisher's exact test. P<0.05 was considered a significant difference.

## Results

*Level of CDKN2B-AS1 was upregulated in the NPC tissues and NPC cell lines*

Compared to the corresponding para-cancerous tissues (n=38), the level of CDKN2B-AS1 was higher in NPC tissues (**Figure 1A**, P<0.05); compared with the normal cell line (NP69), the levels of CDKN2B-AS1 were higher in the NPC cell lines (SUNE-1, 5-8F, 6-10B, HK-1, **Figure 1B**, all P<0.05). We also found that the median survival time of NPC patients with high levels of CDKN2B-AS1 was 60 months, which was shorter than those with low levels of CDKN2B-AS1 (**Figure 1C**, P<0.05). ROC analysis indicated that the area under the curve (AUC) of CDKN2B-AS1 was 0.8373 (**Figure 1D**). According to the ROC curve, the cut-off value was 6.053 (sensitivity + specificity - 100%). Based on the cut-off value, the patients were divided

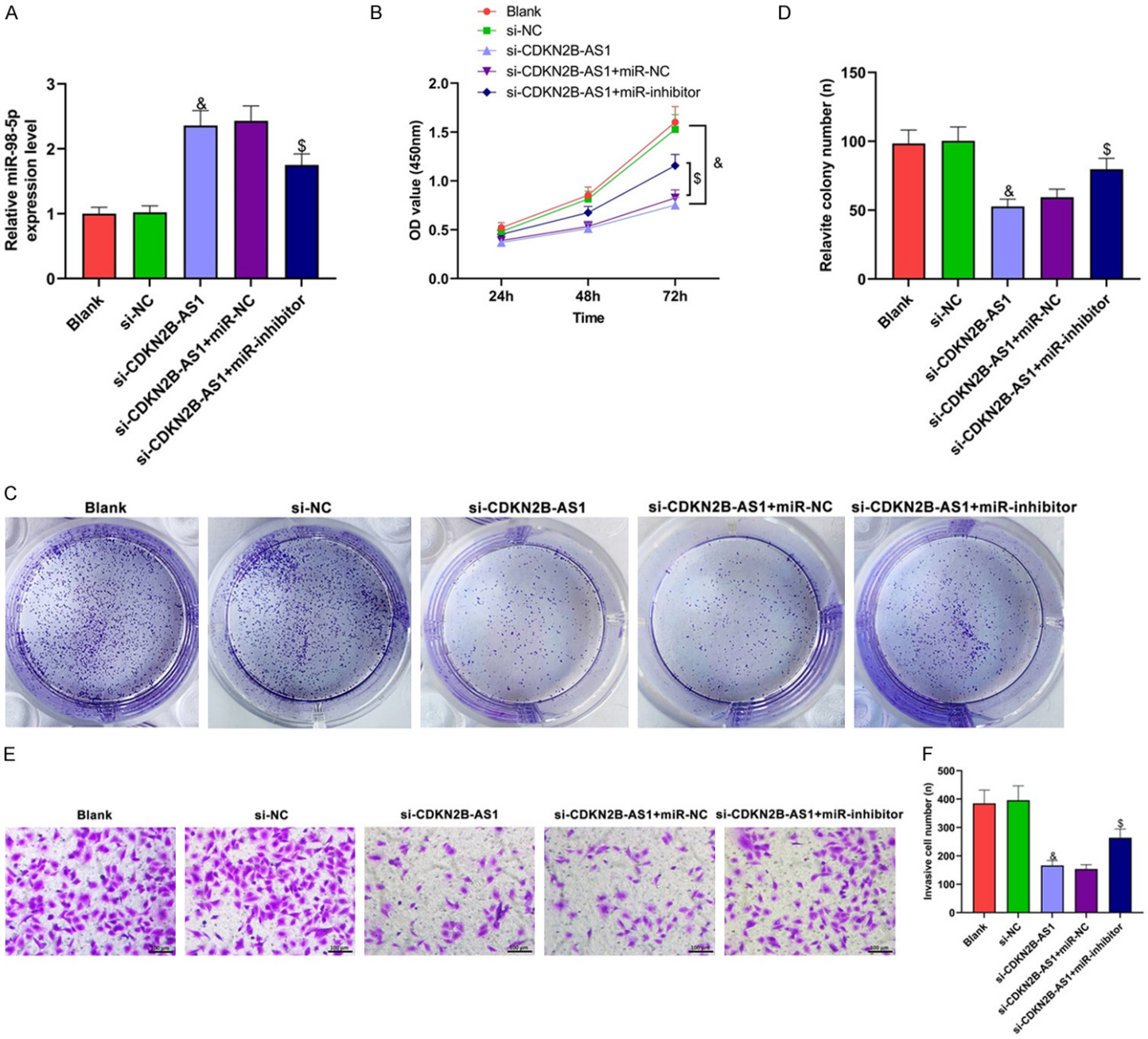
A
Relative miR-98-5p expression level
Blank
si-NC
si-CDKN2B-AS1
si-CDKN2B-AS1+miR-NC
si-CDKN2B-AS1+miR-inhibitor
B
OD value (450nm)
Time
24h
48h
72h
D
Relavite colony number (n)
C
E
F
Invasive cell number (n)

**Figure 4.** The effect of CDKN2B-AS1 on NPC cells could be partially reversed by miR-98-5p. A: Expressions of miR-98-tp in each group detected by qRT-PCR; B: Cell proliferation measured by CCK-8 assay; C, D: Results of clone formation; E, F: Cell invasion measured by Transwell assay (100×). Compared to the si-NC group, $^{\&}$P<0.05. Compared to the CDKN2B-AS1 + miR-NC group, $^{\$}$P<0.05. CDKN2B-AS1: CDKN2B antisense RNA 1; NPC: nasopharyngeal carcinoma; CCK-8: cell counting kit-8; OD: optical density.

into a high expression group (n=31) and the low expression group (n=7). As displayed in **Table 2**, the level of CDKN2B-AS1 was associated with TNM staging, positive VCA-IgA antibody test, and lymph node metastasis in NPC (all P<0.05), indicating that the aberrant expression of CDKN2B-AS1 may participate in the NPC progression.

*CDKN2B-AS1 promoted proliferation, clone formation, and invasion of NPC cells*

The knockdown efficiency of CDKN2B-AS1 was examined. As displayed in **Figure 2A**, the expression of CDKN2B-AS1 decreased significantly in the si-CDKN2B-AS1 group compared with the si-NC group, indicating that CDKN2B-AS1 knockdown was successful. Subsequently, we performed the CCK-8 assay and found that knockdown of CDKN2B-AS1 significantly reduced the proliferation ability of the NPC cells (**Figure 2B**, P<0.05) in comparison with the si-NC group. The colony-forming ability of the cells in the si-CDKN2B-AS1 group was much lower than that in the si-NC group (**Figure 2C**, **2D**, P<0.05). The number of invasive cells in the 5-8F cell line also was reduced substantially by the down-regulation of CDKN2B-AS1 (**Figure 2E**, **2F**). These results suggest that CDKN2B-AS1 can promote the proliferation, clone formation, and invasion of the NPC cells.

*CDKN2B-AS1 functions as ceRNA and competitively sponges miR-98-5p*

During the investigation of the molecular mechanism of CDKN2B-AS1 in NPC pathogenesis, we found that lncRNA could indirectly regulate gene coding by acting as a molecular sponge to absorb miRNA, thereby affecting the downstream gene expression. Thus, we used the starBase and lncRBase tools to predict the miRNAs that might bind to CDKN2B-AS1 (**Figure 3A**). miR-98-5p has been widely studied in different cancers such as lung cancer, prostate cancer, and liver cancer and has been revealed to have an anti-cancer effect [14-16]. However, since there have been no relevant reports on the effect of miR-98-5p in NPC, we aimed to investigate this miRNA in our study.

To clarify the role of CDKN2B-AS1 and miR-98-5p in NPC, we performed a FISH assay and found that the subcellular localization of CDKN2B-AS1 was mainly in the cytoplasm (**Figure 3B**). Several binding sites of miR-98-5p on CDKN2B-AS1 were found using the bioinformatic website (**Figure 3C**). DLR assay showed that compared with the cells transfected with miR-NC and CDKN2B-AS1-wt, the luciferase activity of 293 T cells transfected with CDKN2B-AS1-wt and miR-98-5p mimic was much lower (P<0.05, **Figure 3D**). RIP assay showed that CDKN2B-AS1 and miR-98-5p were markedly enriched in the Ago2 binding group (**Figure 3E**, both P<0.05).

The dbDEMC database showed that miR-98-5p can be highly expressed in the head and neck tumors (**Figure 3F**). However, our study results showed a low level of miR-98-5p in the NPC tissues (**Figure 3G**, P<0.05), and the AUC of miR-98-5p was 0.8293 (**Figure 3H**). The expression of miR-98-5p was negatively correlated with CDKN2B-AS1 in the NPC tissues (**Figure 3I**). The expression of miR-98-5p was downregulated in the NPC cells, whereas the knockdown of CDKN2B-AS1 could increase the expression of miR-98-5p (**Figure 3J**, **3K**, P<0.05). The results confirm that CDKN2B-AS1 is a ceRNA of miR-98-5p, and the aberrant expressions of CDKN2B-AS1 and miR-98-5p are involved in the pathogenesis of NPC.

*miR-98-5p inhibitor partially reverses the effect of silencing CDKN2B-AS1 on NPC*

To investigate the effect of CDKN2B-AS1 regulating miR-98-5p on the NPC cells, si-CDKN2B-AS1 and miR-inhibitor were co-transfected into the 5-8F cells. qRT-PCR showed that the level of miR-98-5p in the si-CDKN2B-AS1 + miR-inhibitor group was lower than that in the si-CDKN2B-AS1 + miR-NC group (**Figure 4A**, P<0.05). CCK-8 assay results demonstrated that compared to the si-CDKN2B-AS1 + miR-NC group, the proliferation ability of the NPC cells increased in the si-CDKN2B-AS1 + miR-inhibitor group (**Figure 4B**, P<0.05). The colony-forming ability of the NPC cells in the si-CDKN2B-

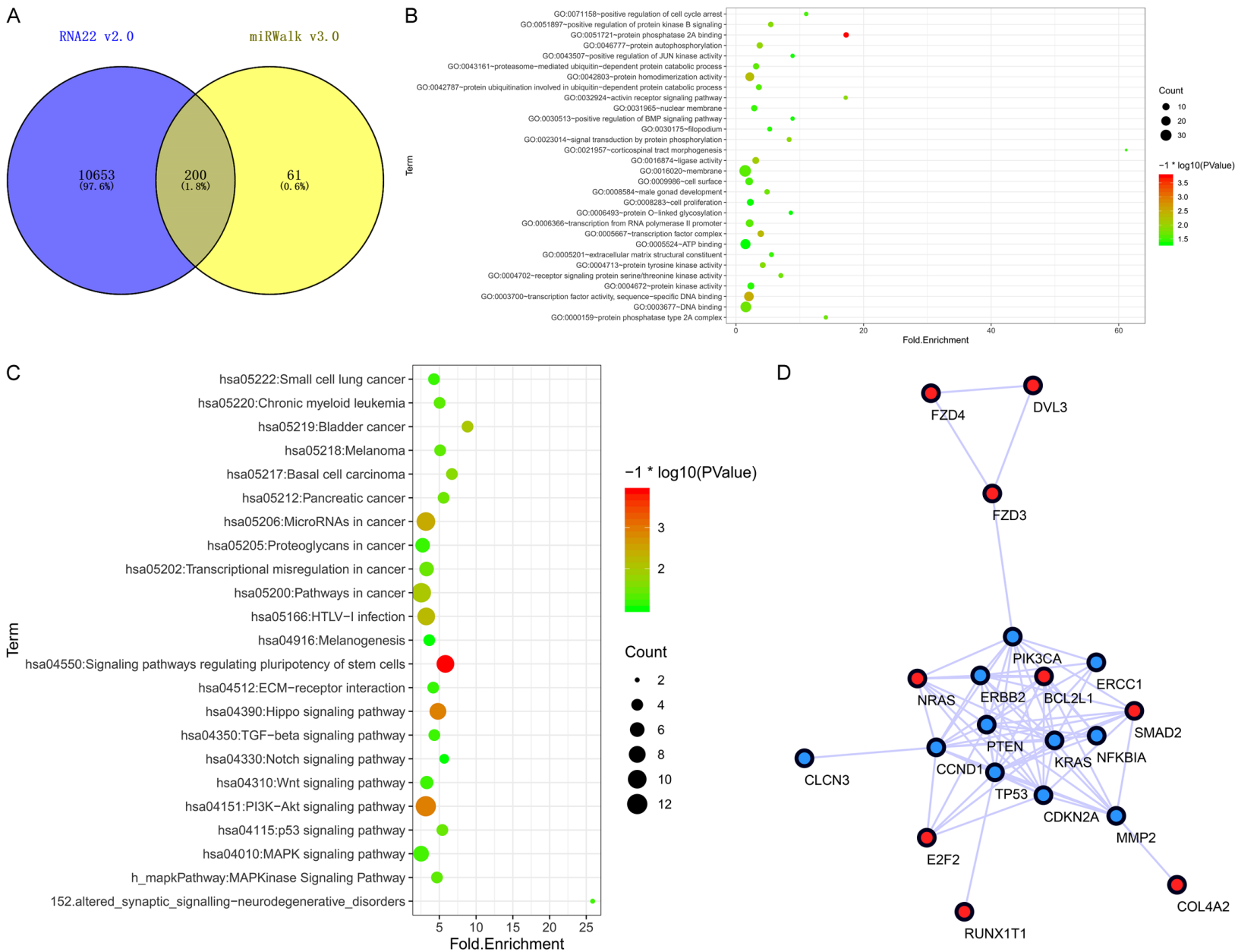
A
RNA22 v2.0
miRWalk v3.0
10653
(97.6%)
200
(1.8%)
61
(0.6%)
B
GO:0071158~positive regulation of cell cycle arrest
GO:0051897~positive regulation of protein kinase B signaling
GO:0051721~protein phosphatase 2A binding
GO:0046777~protein autophosphorylation
GO:0043507~positive regulation of JUN kinase activity
GO:0043161~proteasome-mediated ubiquitin-dependent protein catabolic process
GO:0042803~protein homodimerization activity
GO:0042787~protein ubiquitination involved in ubiquitin-dependent protein catabolic process
GO:0032924~activin receptor signaling pathway
GO:0031965~nuclear membrane
GO:0030513~positive regulation of BMP signaling pathway
GO:0030175~filopodium
GO:0023014~signal transduction by protein phosphorylation
GO:0021957~corticospinal tract morphogenesis
GO:0016874~ligase activity
GO:0016020~membrane
GO:0009986~cell surface
GO:0008584~male gonad development
GO:0008283~cell proliferation
GO:0006493~protein O-linked glycosylation
GO:0006366~transcription from RNA polymerase II promoter
GO:0005667~transcription factor complex
GO:0005524~ATP binding
GO:0005201~extracellular matrix structural constituent
GO:0004713~protein tyrosine kinase activity
GO:0004702~receptor signaling protein serine/threonine kinase activity
GO:0004672~protein kinase activity
GO:0003700~transcription factor activity, sequence-specific DNA binding
GO:0003677~DNA binding
GO:0000159~protein phosphatase type 2A complex
Term
0
20
40
60
Fold.Enrichment
Count
10
20
30
−1 * log10(PValue)
3.5
3.0
2.5
2.0
1.5
C
hsa05222:Small cell lung cancer
hsa05220:Chronic myeloid leukemia
hsa05219:Bladder cancer
hsa05218:Melanoma
hsa05217:Basal cell carcinoma
hsa05212:Pancreatic cancer
hsa05206:MicroRNAs in cancer
hsa05205:Proteoglycans in cancer
hsa05202:Transcriptional misregulation in cancer
hsa05200:Pathways in cancer
hsa05166:HTLV-I infection
hsa04916:Melanogenesis
hsa04550:Signaling pathways regulating pluripotency of stem cells
hsa04512:ECM-receptor interaction
hsa04390:Hippo signaling pathway
hsa04350:TGF-beta signaling pathway
hsa04330:Notch signaling pathway
hsa04310:Wnt signaling pathway
hsa04151:PI3K-Akt signaling pathway
hsa04115:p53 signaling pathway
hsa04010:MAPK signaling pathway
h_mapkPathway:MAPKinase Signaling Pathway
152.altered_synaptic_signalling-neurodegenerative_disorders
Term
5
10
15
20
25
Fold.Enrichment
−1 * log10(PValue)
3
2
Count
2
4
6
8
10
12
D
FZD4
DVL3
FZD3
PIK3CA
ERCC1
NRAS
ERBB2
BCL2L1
SMAD2
PTEN
KRAS
NFKBIA
CLCN3
CCND1
TP53
CDKN2A
MMP2
E2F2
COL4A2
RUNX1T1

**Figure 5.** Targets of CDKN2B-AS1/miR-98-5p. A: The common target genes of miRNA predicted by RNA22, miRDB, Targetscan, and miRWalk; B: Bubble chart of GO enrichment analysis of miRNA target genes; C: Bubble chart of pathway analysis of miRNA target genes; D: Protein interaction network of the candidate genes and the published disease risk genes; candidate genes are indicated by red dots, and disease risk genes are indicated by blue dots. CDKN2B-AS1: CDKN2B antisense RNA 1; GO: gene ontology.

AS1 group was lower than that of the si-NC group, and the colony-forming ability in the si-CDKN2B-AS1 + miR-inhibitor group was higher than that of the si-CDKN2B-AS1 + miR-NC group (**Figure 4C**, **4D**, both P<0.05). Transwell assay showed that the NPC cell invasion ability in the si-CDKN2B-AS1 + miR inhibitor group was greater than that in the si-CDKN2B-AS1 + miR-NC group (**Figure 4E**, **4F**, P<0.05). These results reveal that the effect of CDKN2B-AS1 downregulation on NPC can be partially reversed by miR-98-5p inhibitor.

*Screening of targets of CDKN2B-AS1/miR-98-5p*

RNA22 and miRWalk databases were used to predict the possible downstream targets of miR-98-5p. By controlling the parameters and taking the common results predicted by each tool, we found 200 target genes of miR-98-5p with high reliability (**Figure 5A**). GO and pathway analyses were performed for these 200 genes. The GO analysis showed few significantly enriched GO terms (**Figure 5B**), whereas the pathway analysis showed that high-confidence target genes of miR-98-5p were significantly enriched in cancer-related pathways. Even though the false discovery rates (FDRs) of the differential genes in the cancer-related pathways were not significant, there may be still biologic significance (enrichment: 2.5, P=0.0098, FDR=0.20, **Figure 5C**).

We defined the genes involved in the cancer-related pathway as candidate genes and searched the DisGeNET database (https://www.disgenet.org) for the published NPC (C2931822) risk genes. According to the GDA score, we chose the top 10 disease risk genes as the published high-confidence NPC risk genes and searched the String database to find protein interactions between the candidate genes and the published NPC risk genes. Of the candidate genes, E2F2 was found to have moderate protein interaction with the NPC risk genes (**Figure 5D**), suggesting that miR-98-5p may regulate tumor growth by inhibiting E2F2. Therefore, CDKN2B-AS1 may indirectly upregulate the level of E2F2 by sponging miR-98-5p, thus promoting the occurrence and development of tumor.

*CDKN2B-AS1 regulates miR-98-5p to upregulate E2F2*

By searching the UALCAN database (http://ualcan.path.uab.edu), we observed that the relative expression levels of E2F2 in the head and neck tumors were higher than those in normal head and neck tissues (**Figure 6A**). Our study results showed that compared to normal tissues, E2F2 was highly expressed in NPC tissues (**Figure 6B**, P<0.05). In the 5-8F cell line, E2F2 expression could be downregulated by silencing CDKN2B-AS1 or miR-98-5p overexpression (**Figure 6C**, **6D**, both P<0.05). miR-98-5p knockdown increased E2F2 expression, whereas this effect could be partially reversed by si-CDKN2B-AS1 (**Figure 6E**, P<0.05). Correlation analysis exhibited that the E2F2 level in NPC was negatively correlated with the miR-98-5p level (**Figure 6F**) and was positively correlated with the CDKN2B-AS1 level (**Figure 6G**). The Targetscan website (http://www.targetscan.org/vert72/) helped us to identify the miR-98-5p binding sites on E2F2 (**Figure 6H**). DLR assay displayed that miR-98-5p could significantly reduce the luciferase activity of the vector containing E2F2 wild type 3'UTR sequence, but had no marked effect on vectors containing E2F2 mutant 3'UTR sequence, indicating that miR-98-5p can bind to E2F2 (**Figure 6I**). RIP assay results showed that both E2F2 and miR-98-5p were enriched by Ago2 immunoprecipitation (both P<0.05, **Figure 6J**). These results indicate that E2F2 is a target gene of miR-98-5p, and CDKN2B-AS1 can upregulate E2F2 expression by regulating miR-98-5p.

*E2F2 could partially reverse the effect of miR-98-5p overexpression on NPC cells*

Compared with the miR-NC group, the transfection of miR-98-5p mimic increased the level of miR-98-5p in the 5-8F cells (**Figure 7A**, P<0.05). miR-98-5p mimic was co-transfected with E2F2 or vector, and the level of E2F2 in the miR-98-

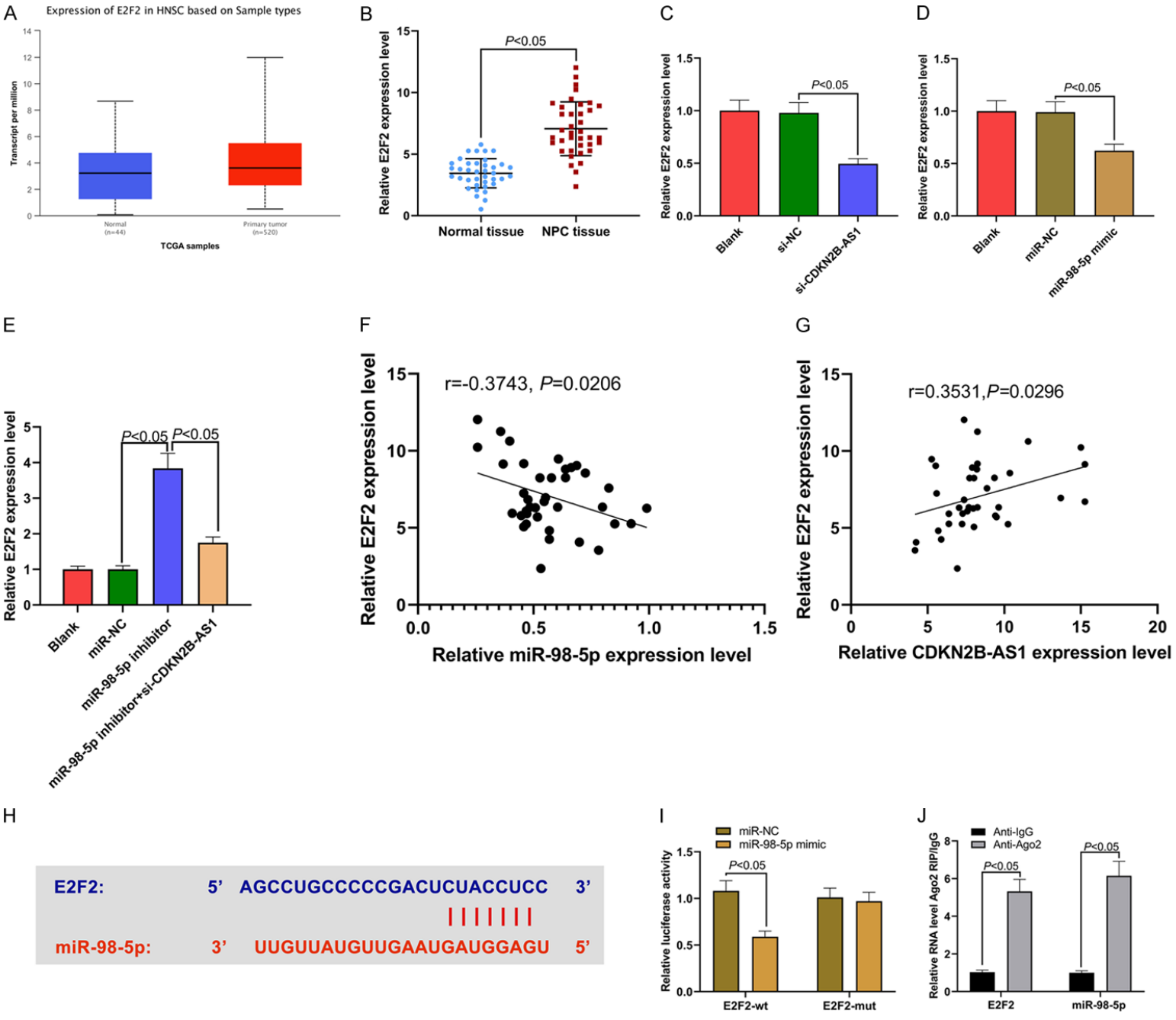
A
Expression of E2F2 in HNSC based on Sample types
Transcript per million
Normal (n=44)
Primary tumor (n=520)
TCGA samples
B
P<0.05
Relative E2F2 expression level
Normal tissue
NPC tissue
C
P<0.05
Relative E2F2 expression level
Blank
si-NC
si-CDKN2B-AS1
D
P<0.05
Relative E2F2 expression level
Blank
miR-NC
miR-98-5p mimic
E
P<0.05 P<0.05
Relative E2F2 expression level
Blank
miR-NC
miR-98-5p inhibitor
miR-98-5p inhibitor+si-CDKN2B-AS1
F
r=-0.3743, P=0.0206
Relative E2F2 expression level
Relative miR-98-5p expression level
G
r=0.3531,P=0.0296
Relative E2F2 expression level
Relative CDKN2B-AS1 expression level
H
E2F2: 5' AGCCUGCCCCCGACUCUACCUCC 3'
miR-98-5p: 3' UUGUUAUGUUGAAUGAUGGAGU 5'
I
miR-NC
miR-98-5p mimic
P<0.05
Relative luciferase activity
E2F2-wt
E2F2-mut
J
Anti-IgG
Anti-Ago2
P<0.05
P<0.05
Relative RNA level Ago2 RIP/IgG
E2F2
miR-98-5p

**Figure 6.** CDKN2B-AS1 sponges miR-98-5p to upregulate E2F2 expression. A: Expression level of E2F2 in head and neck squamous cell carcinoma reported by UALCAN database; B: Expression level of E2F2 in NPC tissues (n=38); C: Effect of silencing CDKN2B-AS1 on E2F2 expression; D: Effect of miR-98-5p overexpression on E2F2; E: Effect of silencing both miR-98-5p and CDKN2B-AS1 on E2F2; F: Correlation of E2F2 expression level with miR-98-5p expression level in NPC; G: Correlation of E2F2 expression level with CDKN2B-AS1 expression level in NPC; H: miR-98-5p binding sites on E2F2; I: DLR assay results; J: RIP assay results. CDKN2B-AS1: CDKN2B antisense RNA 1; NPC: nasopharyngeal carcinoma; OD: optical density; DLR: dual-luciferase reporter; RIP: RNA immunoprecipitation; E2F2: E2F transcription factor 2.

5p mimic + E2F2 group was higher than that in the miR-98-5p mimic + vector group (**Figure 7B**, P<0.05). CCK-8 assay showed that NPC cell proliferation ability decreased markedly in the miR-98-5p mimic group compared with the miR-NC group and increased markedly in the miR-98-5p mimic + E2F2 group compared with the miR-98-5p mimic + vector group (**Figure 7C**, both P<0.05). The colony-forming ability of the NPC cells inhibited in the miR-98-5p mimic + vector group were partially reversed in the miR-98-5p mimic + E2F2 group (**Figure 7D**, **7E**, P<0.05). Transwell assay indicated that the NPC cell invasion ability in the miR-98-5p mimic + E2F2 group was greater than that in the miR-98-5p mimic group (**Figure 7F**, **7G**, P<0.05). Therefore, the effect of miR-98-5p overexpression on NPC could be partially reversed by E2F2.

## Discussion

Evidence has demonstrated that aberrant expression of lncRNA and miRNA play important roles in the occurrence and progression of various cancers [18-20]. Through searching the database and conducting experiments, we found that lncRNA CDKN2B-AS1 expression was significantly upregulated, whereas the miR-98-5p expression was downregulated in the NPC tissues and cells. CDKN2B-AS1 could enhance E2F2 expression through sponging miR-98-5p, thus promoting the proliferation, invasion, and clone formation of NPC cells. These findings suggest that CDKN2B-AS1, miR-98-5p, and E2F2 serve essential roles in regulating the pathogenesis of NPC and can be used as prognostic markers for NPC.

Clinically, the anatomy-based TNM staging system cannot accurately predict the risks of recurrence and tumor metastasis in NPC patients [21, 22]. Therefore, it is critical to find biomarkers that can predict the occurrence and prognosis of NPC and affect the progression of cancer. Increasing evidence supports the idea of constructing a lncRNA-miRNA-mRNA interaction network in order to identify regulatory factors related to the prognosis of cancer patients and provide novel molecular markers for cancer treatment, which should help develop a personalized treatment for patients [23, 24]. In this study, we identified that CDKN2B-AS1 can act as a ceRNA of miR-98-5p to regulate E2F2 expression, thereby participating in the pathogenesis of NPC.

Previous studies have reported that the overexpression of CDKN2B-AS1 can promote the growth of NPC [11, 12]. In the present study, we observed that the expression of CDKN2B-AS1 was increased in NPC, and the survival rate of NPC patients with high expression of CDKN2B-AS1 was lower. CDKN2B-AS1 can promote the proliferation, invasion, and clonal formation of NPC cells, thus working as a tumor-promoting factor in NPC.

LncRNAs have been demonstrated to be able to regulate the expression and activity of miRNAs in recent years [25, 26]. In this study, we used the starBase and lncRBase to predict the miRNA that targets CDKN2B-AS1 and selected mir-98-5p. Since miR-98-5p is downregulated in a variety of tumors and works as a tumor suppressor, we speculated that miR-98-5p may also have an antitumor effect in NPC [14-16]. In this study, we found that miR-98-5p was downregulated in NPC, which inhibited the proliferation, invasion, and clone formation of NPC cells. Moreover, CDKN2B-AS1 could negatively regulate the level of miR-98-5p in NPC, and miR-98-5p could partially reverse the ability of CDKN2B-AS1 to promote the malignant progression of NPC. These results indicate that CDKN2B-AS1 promotes NPC progression by sponging miR-98-5p, and miR-98-5p acts as a tumor suppressor in NPC.

The function of lncRNA, a ceRNA, normally depends on the binding sites on miRNAs [27, 28]. In this study, we first predicted the down-

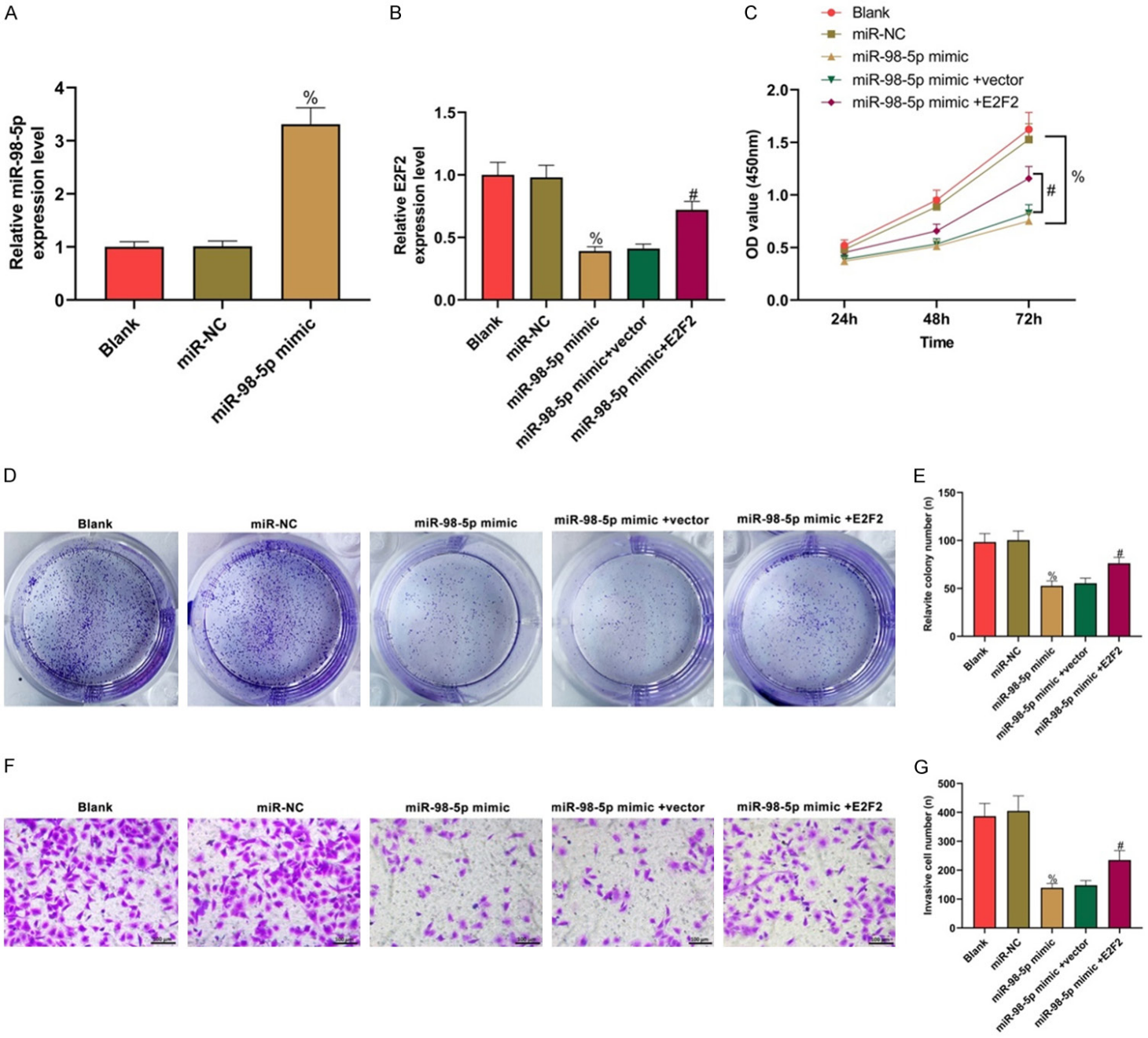
A
Relative miR-98-5p expression level
%
Blank
miR-NC
miR-98-5p mimic
B
Relative E2F2 expression level
%
#
Blank
miR-NC
miR-98-5p mimic
miR-98-5p mimic+vector
miR-98-5p mimic+E2F2
C
Blank
miR-NC
miR-98-5p mimic
miR-98-5p mimic +vector
miR-98-5p mimic +E2F2
OD value (450nm)
%
#
24h
48h
72h
Time
D
Blank
miR-NC
miR-98-5p mimic
miR-98-5p mimic +vector
miR-98-5p mimic +E2F2
E
Relavite colony number (n)
F
Blank
miR-NC
miR-98-5p mimic
miR-98-5p mimic +vector
miR-98-5p mimic +E2F2
G
Invasive cell number (n)

**Figure 7.** Effect of miR-98-5p overexpression on NPC cells was partially reversed by E2F2. A, B: Expressions of miR-98-5p and E2F2 in each group determined by qRT-PCR; C: Cell proliferation measured by CCK-8 assay; D, E: Results of clone formation; F, G: Cell invasion measured by Transwell assay (100×). Compared with the miR-NC group, $^{\%}P<0.05$; compared with the miR-98-5p mimic + vector group, $^{\#}P<0.05$. CCK-8: cell counting kit-8; OD: optical density; E2F2: E2F transcription factor 2.

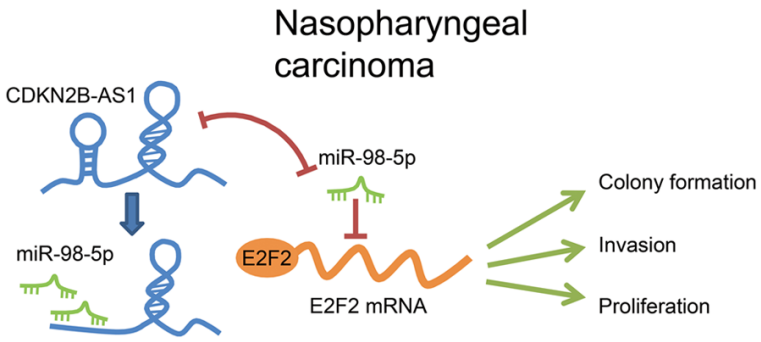


**Figure 8.** Mechanism of the regulation of CDKN2B-AS1 through miR-98-5p/E2F2 axis in NPC progression. CDKN2B-AS1: CDKN2B antisense RNA 1; NPC: nasopharyngeal carcinoma; E2F2: E2F transcription factor 2.

stream target genes of miR-98-5p using several databases and then conducted GO and pathway analysis to search for the genes that can be studied. We identified that high-confidence target genes of miR-98-5p were significantly enriched in the cancer-related pathways. In this pathway, we found E2F2, a regulatory factor in cell cycle, cellular apoptosis, and DNA damage, as a target gene. E2F2 is related to poor prognosis of patients with various malignant tumors, including gastric cancer, breast cancer, and non-small cell lung cancer [29-31]. In addition, E2F2 has been widely studied in NPC. Some studies have demonstrated that E2F2, as a tumor-promoting factor, participates in the proliferation and metastasis of NPC regulated by PPAR-γ, and NPC is also regulated by the E2F2 pathway [32-34]. Databases show that the levels of E2F2 in head and neck tumors are much higher than those in normal head and neck tissues. We confirmed that E2F2 is a downstream target gene of miR-98-5p using DLR assay and RIP assay. In addition, E2F2 expression in NPC was positively correlated with CDKN2B-AS1. Overexpressing miR-98-5p inhibited E2F2 mRNA expression, whereas silencing miR-98-5p and downregulating CDKN2B-AS1 resulted in decreased expression of E2F2, suggesting that CDKN2B-AS1 can competitively bind to miR-98-5p to regulate E2F2 expression. The inhibitory effect of miR-98-5p overexpression on the proliferation, invasion, and clone formation of NPC cells could be partially reversed by the upregulation of E2F2 expression. All these findings indicate that the CDKN2B-AS1/miR-98-5p/E2F2 axis may be a key pathway in regulating the proliferation, invasion, and clone formation of NPC cells.

In conclusion, CDKN2B-AS1 is an NPC-inducing factor. CDKN2B-AS1, as a ceRNA, can sponge miR-98-5p to upregulate E2F2 expression, thereby promoting the proliferation, invasion, and clone formation of NPC cells (**Figure 8**). However, the sample size in our experiment was small and in vivo experiment was not performed to verify the effect of CDKN2B-AS1/miR-98-5p/E2F on NPC. Moreover, other possible signaling molecules and pathways regulated by CDKN2B-AS1/miR-98-5p/E2F2 CDKN2B-AS1/miR-98-5p/E2F in NPC need to be further investigated.

CDKN2B-AS1/miR-98-5p/E2F2 axis plays an essential role in the occurrence and progression of NPC, which may be a treatment target and prognostic marker for NPC patients.

## Disclosure of conflict of interest

None.

**Address correspondence to:** Jiaxiong Zhang and Wentao Zou, Department of Otorhinolaryngology, Shanghai Tenth Peoples' Hospital, Tongji University, No. 301 Middle Yanchang Road, Shanghai 200072, China. Tel: +86-18917683317; E-mail: zhangjiaxiong002@163.com (JXZ); Tel: +86-13585633971; E-mail: zouwentao002@126.com (WTZ)

## References

[1] Zhang S, Yang S, Xu P, Xu Y, Zhou G, Ou X, Wu R, Lan M, Fontanarosa D, Dowling J, Wang X, Lin S, Yi JL, Sun Y, Hu C and Lang J. Variations of clinical target volume delineation for primary site of nasopharyngeal cancer among five centers in China. Front Oncol 2020; 10: 1572.

[2] Chan SK, Chan SY, Choi HC, Tong CC, Lam KO, Kwong DL, Vardhanabhuti V, Leung TW, Luk MY, Lee AW and Lee VH. Prognostication of half-life clearance of plasma EBV DNA in previously untreated non-metastatic nasopharyngeal carcinoma treated with radical intensity-modulated radiation therapy. Front Oncol 2020; 10: 1417.
[3] Guan S, Wei J, Huang L and Wu L. Chemotherapy and chemo-resistance in nasopharyngeal carcinoma. Eur J Med Chem 2020; 207: 112758.
[4] Chen X, Liang R and Zhu X. Anti-EGFR therapies in nasopharyngeal carcinoma. Biomed Pharmacother 2020; 131: 110649.
[5] Tseng M, Ho F, Leong YH, Wong LC, Tham IW, Cheo T and Lee AW. Emerging radiotherapy technologies and trends in nasopharyngeal cancer. Cancer Commun (Lond) 2020; 40: 395-405.
[6] Huang SH and O'Sullivan B. Overview of the 8th edition TNM classification for head and neck cancer. Curr Treat Options Oncol 2017; 18: 40.
[7] Wang Y, Zhou L, Lu J, Jiang B, Liu C, Guo J and Xiao GG. Research progress on long non-coding RNAs and their roles as potential biomarkers for diagnosis and prognosis in pancreatic cancer. Cancer Cell Int 2020; 20: 457.
[8] Xiao Y, Xiao T, Ou W, Wu Z, Wu J, Tang J, Tian B, Zhou Y, Su M and Wang W. LncRNA SNHG16 as a potential biomarker and therapeutic target in human cancers. Biomark Res 2020; 8: 41.
[9] Wang S, You H and Yu S. Long non-coding RNA HOXA-AS2 promotes the expression levels of hypoxia-inducible factor-1α and programmed death-ligand 1, and regulates nasopharyngeal carcinoma progression via miR-519. Oncol Lett 2020; 20: 245.
[10] Meng XJ, Wang JC, Wang AQ and Xia WQ. Downregulation of lncRNA CCHE1 inhibits cell proliferation, migration and invasion by suppressing MEK/ERK/c-MYC pathway in nasopharyngeal carcinoma. Eur Rev Med Pharmacol Sci 2020; 24: 8880-8888.
[11] Pasmant E, Sabbagh A, Vidaud M and Bièche I. ANRIL, a long, noncoding RNA, is an unexpected major hotspot in GWAS. FASEB J 2011; 25: 444-448.
[12] Bei JX, Li Y, Jia WH, Feng BJ, Zhou G, Chen LZ, Feng QS, Low HQ, Zhang H, He F, Tai ES, Kang T, Liu ET, Liu J and Zeng YX. A genome-wide association study of nasopharyngeal carcinoma identifies three new susceptibility loci. Nat Genet 2010; 42: 599-603.
[13] Zou ZW, Ma C, Medoro L, Chen L, Wang B, Gupta R, Liu T, Yang XZ, Chen TT, Wang RZ, Zhang WJ and Li PD. LncRNA ANRIL is up-regulated in nasopharyngeal carcinoma and promotes the cancer progression via increasing proliferation, reprograming cell glucose metabolism and inducing side-population stem-like cancer cells. Oncotarget 2016; 7: 61741-61754.
[14] Zhou DH, Wang X and Feng Q. EGCG enhances the efficacy of cisplatin by downregulating hsa-miR-98-5p in NSCLC A549 Cells. Nutr Cancer 2014; 66: 636-644.
[15] Moya L, Meijer J, Schubert S, Matin F and Batra J. Assessment of miR-98-5p, miR-152-3p, miR-326 and miR-4289 expression as biomarker for prostate cancer diagnosis. Int J Mol Sci 2019; 20: 1154.
[16] Shen Q, Jiang S, Wu M, Zhang L, Su X and Zhao D. LncRNA HEIH confers cell sorafenib resistance in hepatocellular carcinoma by regulating miR-98-5p/PI3K/AKT pathway. Cancer Manag Res 2020; 12: 6585-6595.
[17] Liu X and Hu C. Novel potential therapeutic target for E2F1 and prognostic factors of E2F1/2/3/5/7/8 in human gastric cancer. Mol Ther Methods Clin Dev 2020; 18: 824-838.
[18] Yang Y, Yujiao W, Fang W, Linhui Y, Ziqi G, Zhichen W, Zirui W and Shengwang W. The roles of miRNA, lncRNA and circRNA in the development of osteoporosis. Biol Res 2020; 53: 40.
[19] Taheri M, Eghtedarian R, Dinger ME and Ghafouri-Fard S. Dysregulation of non-coding RNAs in autoimmune thyroid disease. Exp Mol Pathol 2020; 117: 104527.
[20] Ghafouri-Fard S, Shoorei H and Taheri M. Role of non-coding RNAs in the pathogenesis of endometriosis. Front Oncol 2020; 10: 1370.
[21] Huang W, Shi G, Yong Z, Li J, Qiu J, Cao Y, Zhao Y and Yuan L. Downregulation of RKIP promotes radioresistance of nasopharyngeal carcinoma by activating NRF2/NQO1 axis via downregulating miR-450b-5p. Cell Death Dis 2020; 11: 504.
[22] Yang Q, Guo Y, Ou X, Wang J and Hu C. Automatic T Staging using weakly supervised deep learning for nasopharyngeal carcinoma on MR images. J Magn Reson Imaging 2020; 52: 1074-1082.
[23] Zhang Q, Liang Y, Yuan H, Li S, Wang JB, Li XM, Tao JH, Pan HF and Ye DQ. Integrated analysis of lncRNA, miRNA and mRNA expression profiling in patients with systemic lupus erythematosus. Arch Med Sci 2019; 15: 872-879.
[24] Hu H, Jia Q, Xi J, Zhou B and Li Z. Integrated analysis of lncRNA, miRNA and mRNA reveals novel insights into the fertility regulation of large white sows. BMC Genomics 2020; 21: 636.
[25] Deng J, Zeng W, Kong W, Shi Y and Mou X. The study of sarcoma microenvironment heteroge-

neity associated with prognosis based on an immunogenomic landscape analysis. Front Bioeng Biotechnol 2020; 8: 1003.
[26] Sun CY, Zhang XP, Liu F and Wang W. Orchestration of lincRNA-p21 and miR-155 in modulating the adaptive dynamics of HIF-1α. Front Genet 2020; 11: 871.
[27] Yang T, Li N, Hou R, Qiao C and Liu C. Development and validation of a four-microrna signature for placenta accreta spectrum: an integrated competing endogenous RNA network analysis. Ann Transl Med 2020; 8: 919.
[28] Ou YH, Liu YK, Zhu LQ, Chen MQ, Yi XC, Chen H and Zhang JP. LncRNA and transcriptomic analysis of fetal membrane reveal potential targets involved in oligohydramnios. BMC Med Genomics 2020; 13: 137.
[29] Yang C, Zhang ZC, Liu TB, Xu Y, Xia BR and Lou G. E2F1/2/7/8 as independent indicators of survival in patients with cervical squamous cell carcinoma. Cancer Cell Int 2020; 20: 500.
[30] Bellat V, Verchère A, Ashe SA and Law B. Transcriptomic insight into salinomycin mechanisms in breast cancer cell lines: synergistic effects with dasatinib and induction of estrogen receptor β. BMC Cancer 2020; 20: 661.
[31] Bai Q, Li L, Chen F, Zhu J, Cao L, Yang Y and Zhong F. Suppression of circular RNA Hsa_circ_0109320 attenuates non-small cell lung cancer progression via MiR-595/E2F7 axis. Med Sci Monit 2020; 26: e921200.
[32] Yang PL, Wang JS, Cheng XM, Chen JC, Zhu H, Li XL, Cao L and Tang W. PPAR-γ ligand inhibits nasopharyngeal carcinoma cell proliferation and metastasis by regulating E2F2. PPAR Res 2019; 2019: 8679271.
[33] Yang Y, Liao Q, Wei F, Li X, Zhang W, Fan S, Shi L, Li X, Gong Z, Ma J, Zhou M, Xiang J, Peng S, Xiang B, Deng H, Yang Y, Li Y, Xiong W, Zeng Z and Li G. LPLUNC1 inhibits nasopharyngeal carcinoma cell growth via down-regulation of the MAP kinase and cyclin D1/E2F pathways. PLoS One 2013; 8: e62869.
[34] Niu Z, Liu H, Zhou M, Wang H, Liu Y, Li X, Xiong W, Ma J, Li X and Li G. Knockdown of c-Myc inhibits cell proliferation by negatively regulating the Cdk/Rb/E2F pathway in nasopharyngeal carcinoma cells. Acta Biochim Biophys Sin (Shanghai) 2015; 47: 183-191.